

See discussions, stats, and author profiles for this publication at: <https://www.researchgate.net/publication/239030510>

Fluorescence Anisotropy of 2,5,8,11-Tetra-tert-butylperylene (I) and 2,5,10,13-Tetra-tert-butylterrylene (II) in Alkanes and Alcohols

ARTICLE *in* THE JOURNAL OF PHYSICAL CHEMISTRY · JANUARY 1996

Impact Factor: 2.78 · DOI: 10.1021/jp9517108

CITATIONS

35

READS

15

6 AUTHORS, INCLUDING:



GB Dutt

Bhabha Atomic Research Centre

75 PUBLICATIONS 1,632 CITATIONS

SEE PROFILE



Marcel Ameloot

Hasselt University

220 PUBLICATIONS 3,488 CITATIONS

SEE PROFILE



Frans C De Schryver

University of Leuven

670 PUBLICATIONS 21,225 CITATIONS

SEE PROFILE

Fluorescence Anisotropy of 2,5,8,11-Tetra-*tert*-butylperylene and 2,5,10,13-Tetra-*tert*-butylterrylene in Alkanes and Alcohols

Steven De Backer,[†] G. Bhaskar Dutt,[†] Marcel Ameloot,[‡] Frans C. De Schryver,^{*,†} Klaus Müllen,[§] and Frank Holtrup[§]

Department of Chemistry, Katholieke Universiteit Leuven, Celestijnenlaan 200F, 3001 Heverlee, Belgium; Limburgs Universitair Centrum, Universitaire Campus, 3590 Diepenbeek, Belgium; and Max-Planck-Institut für polymerforschung, Ackermanweg 10, W-6500 Mainz, Germany

Received: June 19, 1995; In Final Form: September 22, 1995[®]

The fluorescence anisotropy of two neutral and nonpolar molecules, 2,5,8,11-tetra-*tert*-butylperylene (TP) and 2,5,10,13-tetra-*tert*-butylterrylene (TT), is studied in a series of *n*-alcohols and alkanes. Both probes show an absorption band in the UV region and one in the visible region. The polarized fluorescence decay traces are globally analyzed over different excitation wavelengths. TP and TT can be modeled as oblate ellipsoids with essentially identical rotational correlation times. The anisotropy decay can well be approximated by a monoexponential model for both solvent series. The rotational correlation times (ϕ) vary linearly with viscosity (η) for both solvent series. Higher values for ϕ/η are reached in alkanes than in alcohols, the effect being more pronounced for TP than for TT. The predictions of the quasihydrodynamic models of Gierer–Wirtz and of Dote–Kivelson–Schwartz (DKS) are compared to the experimental data. Only the DKS model can predict qualitatively the experimental observations. The difference in rotational correlation times can be explained in terms of the higher free volume in alcohols than in alkanes. Anisotropy decay measurements of TT in hexadecane and decanol in the temperature range 25–60 °C give additional support to the applicability of the DKS theory for nonpolar solutes and suggest that an Arrhenius formalism to calculate the activation energy for rotation from the SDE equation is not appropriate when solute and solvent molecules are of similar magnitude.

1. Introduction

The rotational diffusion of solutes is well described by the theory of Brownian motion if the molecule is sufficiently large as compared to the solvent molecules. In the approximation that the solvent can be considered as a structureless continuum, the rotational correlation time, ϕ , of the solute is given by the so called Stokes–Debye–Einstein (SDE) equation

$$\phi = \eta V C f / kT \quad (1)$$

with η the solvent viscosity, V the volume of the solute, k the Boltzmann constant, and T the absolute temperature. The factor f , called the shape factor, introduced by Perrin,¹ corrects for the shape of the rotating molecule if the molecule is not spherical. C is a measure of the coupling between the rotating molecule and the solvent molecules. The upper limit corresponds to a strong interaction or sticking boundary conditions ($C = 1$) while the lower limit supposes no interaction or slipping boundary conditions.^{2,3} Sticking boundary conditions are expected for probe molecules whose size is considerably larger than that of the solvent molecules, while the slipping limit describes the motion of solute molecules whose size is comparable to or less than that of the solvent molecules. However, some experimental rotational correlation times seem to be lower than this lower limit^{4,5} (slip boundary conditions). In order to explain this discrepancy, it becomes necessary to

invoke the molecularity of the system. The Gierer–Wirtz (GW) model⁶ takes into account the relative sizes of the solute and solvent molecules to calculate the appropriate value for the C factor,

$$C = \sigma_{\text{GW}} C_0 \quad (2)$$

with

$$\sigma_{\text{GW}} = \frac{1}{1 + 6(V_s/V_p)^{1/3}} \quad (3)$$

$$C_0 = \left[\frac{6(V_s/V_p)^{1/3}}{(1 + 2(V_s/V_p)^{1/3})^4} + \frac{1}{(1 + 4(V_s/V_p)^{1/3})^3} \right]^{-1} \quad (4)$$

where V_s and V_p refer to the volume of the solvent and the probe, respectively. These equations do not take into account the degree of contact between probe and solvent which can change from solvent to solvent due to the free spaces between the solvent molecules. To correct for these free spaces, Dote, Kivelson, and Schwartz (DKS)⁷ proposed the following equations to calculate the C factor

$$C = (1 + \gamma/\varphi)^{-1} \quad (5)$$

$$\varphi = \phi_{\text{slip}}/\phi_{\text{SDE}} \quad (6)$$

ϕ_{slip} corresponds to the rotational correlation time of the solute as predicted by the slip hydrodynamics, and ϕ_{SDE} corresponds to the rotational correlation time predicted by the SDE relation for a sphere with the same volume as the solute molecule. The

* To whom correspondence should be addressed.

[†] Katholieke Universiteit Leuven.

[‡] Limburgs Universitair Centrum.

[§] Max-Planck-Institut für polymerforschung.

[®] Abstract published in *Advance ACS Abstracts*, December 1, 1995.

factor γ is defined as

$$\gamma = \left(\frac{Bk_B T \kappa_T \eta}{V_P} \right) [4(V_P/V_S)^{2/3} + 1] \quad (7)$$

where B is the Hildebrand–Batchinski parameter and κ_T the isothermal compressibility of the solvent.

Previous rotational reorientation studies^{8–11} have often stressed the approximate validity of the hydrodynamic SDE model. The questionable validity of this model may be obscured by the adjustment of parameters characterizing the size and shape of the solute or the boundary conditions.¹² A number of authors compared the rotational diffusion of apolar probes in alkanes and alcohols.^{13–15} They all observed a faster diffusion in alcohols than in alkanes for the same η/T ratio. As the volume of the solute increases, the difference between the ϕ values measured in the two solvent series decreases, and the rotational correlation times tend to the stick limit. Both theories (GW and DKS), however, fail to predict the transition toward sticking boundary conditions as the solute size increases. The GW theory is unable to predict the observed faster rotation in alcohols, while the DKS theory predicts qualitatively this experimental observation because of the higher free volume in alcohols than in alkanes. A good correlation is found between calculated values according to the DKS theory and experimental data up to a solute radius of 4.5 Å. To obtain more experimental data in this region of solute radii, Roy et al.¹⁵ studied a series of quater- and quinquephenyl compounds having radii between 4 and 5 Å. These compounds are modeled as prolate ellipsoids. Roy et al.¹⁵ suggest that it would be interesting to study a series of oblate ellipsoids to supplement the data in this volume region. To this aim the fluorescence anisotropy of 2,5,8,11-tetra-*tert*-butylperylene (TP) and 2,5,10,13-tetra-*tert*-butylterrylene (TT) is investigated, since they could, on the basis of molecular models, behave as oblates (Figure 1). These molecules are rigid and differ only in aspect ratio while the interaction with the solvent is unchanged. Since both molecules are apolar, no interference of dielectric friction or superstick can be expected. Furthermore, TP and TT can be excited in two different bands, so that different angles between absorption and emission dipoles can be utilized. This leads to an enhanced discrimination power between different anisotropy models.¹⁶ Additional advantage of the use of TP and TT is that the parameters that describe the fluorescence anisotropy decay of perylene are well-known.^{16–20}

2. Theory

The time-dependent fluorescence anisotropy, $r(t)$, is defined as

$$r(t) = \frac{i_{\parallel}(t) - i_{\perp}(t)}{i_{\parallel}(t) + 2i_{\perp}(t)} \quad (8)$$

where i_{\parallel} and i_{\perp} denote respectively the polarized fluorescence decays with the emission polarizers set parallel and perpendicular to the polarization direction of the excitation light, which is perpendicular to the excitation-detection plane. The analytical expression for $r(t)$ for a general ellipsoid contains at most five exponentials.²¹ This expression reduces to one exponential for spheres and three exponentials for ellipsoids with a symmetry axis. When a transition moment is parallel to the symmetry axis, the anisotropy decay can be described by a single correlation time. However, when the transition moment is perpendicular to the symmetry axis, two correlation times are necessary to describe the anisotropy decay.^{22,23} For an oblate molecule with transition dipoles perpendicular to the axis of

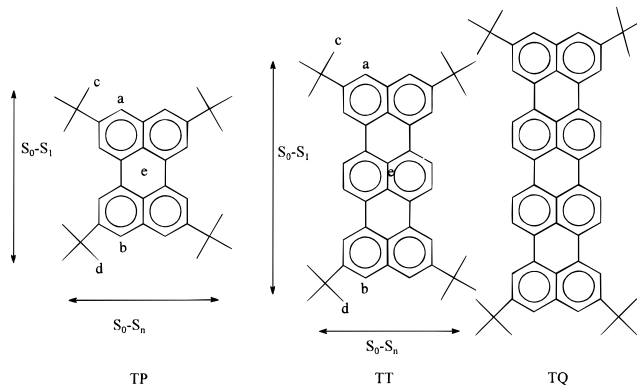


Figure 1. Molecular structures of TP, TT, and TQ.

symmetry $r(t)$ is given by¹⁷

$$r(t) = 0.1e^{-t/\phi_1} + 0.3 \cos 2\alpha e^{-t/\phi_2} \quad (9)$$

$$\phi_1 = 1/6D_{\perp} \quad (10)$$

$$\phi_2 = 1/(2D_{\perp} + 4D_{\parallel}) \quad (11)$$

where D_{\perp} and D_{\parallel} refer to the diffusion coefficients for rotation about an axis perpendicular and parallel to the axis of symmetry, respectively. However, it is difficult to resolve these two rotational correlation times under sticking boundary conditions.²⁴ Only under slipping boundary conditions is there a chance to resolve both rotational motions.¹⁶ α is the angle between absorption and emission dipole. The limiting anisotropy is defined as²⁵

$$r_0 = 0.4 \left(\frac{3 \cos^2 \alpha - 1}{2} \right) \quad (12)$$

3. Materials and Methods

Materials. The synthesis of the compounds has been described previously.²⁶ All solvents were analytical grade. All solutions used in the depolarization measurements have an absorbance lower than 0.1, corresponding to a concentration less than 10^{-5} M.

Instrumentation. The absorption spectra are measured at 20 ± 1 °C with a Perkin-Elmer Lambda 6 UV–vis spectrophotometer.

Steady-state fluorescence spectra are measured with an SLM-8000C spectrofluorimeter in L-format. The anisotropy spectra $\langle r(\lambda_{em}) \rangle$ are corrected for the bias in the detection system via the equation

$$\langle r(\lambda_{em}) \rangle = \frac{I_{VV}(\lambda_{em}) - G(\lambda_{em}) I_{VH}(\lambda_{em})}{I_{VV}(\lambda_{em}) + 2G(\lambda_{em}) I_{VH}(\lambda_{em})} \quad (13)$$

where G is an instrumental factor given by

$$G(\lambda_{em}) = \frac{I_{HV}(\lambda_{em})}{I_{HH}(\lambda_{em})} \quad (14)$$

In these equations I stands for the fluorescence intensity, and the first and second subscripts refer to the settings of the excitation and emission polarizers, respectively. V and H denote the vertical and horizontal orientation, respectively.

The temperature, monitored inside the cuvette, is controlled by a Lauda RUL 480 thermostat–cryostat using a RPt100 resistor.

The polarized emission decays are obtained by the single-photon timing technique. TP is excited at 423 nm by the

TABLE 1: Linking Scheme in the Global Analysis for Different Experimental Conditions for One Reference Compound^a

	α	τ	β	ϕ	κ	τ_{ref}
polarizer setting	+	+	+	+	—	+
time increment	—	+	+	+	—	+
excitation wavelength	—	(+)	—	+	—	(+)
emission wavelength	—	+	+	+	—	+
temperature	—	—	+	—	—	—
solvent	—	—	+	—	—	+

^a Symbols: +, this parameter can be linked by changing the experimental condition; —, this parameter cannot be linked by changing the experimental condition; (+), a slight improvement of the statistical criteria is observed when this parameter is not linked (see text).

polarized output of a titanium-sapphire laser, pumped by a beam-locked argon ion laser at 488 nm. Diodecylloxacarbocyanine (TBO) in ethanol ($\tau = 0.2$ ns) is used as reference compound. The UV band of TP is excited at 271 nm using the frequency-doubled output of a pyromethane dye laser, pumped by a beam-locked argon ion laser at 514 nm. 1,4-Bis(5-phenyloxazol-2-yl)benzene (POPOP) in methylcyclohexane ($\tau = 1.15$ ns) is used as reference compound. The same setup is used to excite TT at 271 and 540 nm (undoubled). Cresyl violet in water ($\tau = 2.08$ ns) is used as a reference compound at both excitation wavelengths. In the temperature study of TT erythrosine in methanol ($\tau = 0.48$ ns) is used as a reference compound. The repetition frequency of the excitation pulses is 800 kHz. All the decay traces have 511 channels. The number of counts in the peak channel is around 10^4 . The fluorescence photons are detected by a microchannel plate (Hamamatsu R2809U). The full width at half-maximum of the instrument response function is typically around 50 ps.

Data Analysis. The fluorescence intensity decays, $i(\theta, t)$, are collected at three different orientations, θ , of the emission polarizer (0° , 54.7° , 90°). These decays are simultaneously analysed using a global analysis fitting program²⁷ according to

$$i(\theta, t) = [\kappa(\theta)/3]\alpha \exp(-t/\tau)[1 + (3 \cos^2 \theta - 1) \times \sum_{j=1}^m \beta_j \exp(-t/\phi_j)] \quad (15)$$

where τ represents the fluorescence decay time and ϕ_j the rotational correlation times of the fluorophore. $\kappa(\theta)$ is a matching factor. The program offers the possibility to keep selected fitting parameters constant or to keep the sum of the β_j constant at a given value. Since the values of the β_j are characteristic for a fluorophore and independent of the solvent, it is possible to link these parameters over the different solvents but not over different excitation wavelengths.²⁸ The rotational correlation times can be linked over different excitation wavelengths but not over the various solvents. The possible linking schemes with respect to the various experimental conditions are shown in Table 1.

The program uses reference convolution and the reference lifetime, τ_{ref} , is in all cases freely adjustable. The fitting parameters are determined by minimizing the global reduced χ_g^2 ,

$$\chi_g^2 = \sum_k \sum_i w_{ki} (I_{ki}^o - I_{ki}^c)^2 / \nu \quad (16)$$

where the index k sums over q experiments, the index i sums over the appropriate channel limits for each individual experiment, and w_{ki} are the weighting factors. I_{ki}^o and I_{ki}^c denote respectively the observed and calculated values corresponding to the i th channel of the k th experiment. ν represents the number

TABLE 2: Limiting Anisotropy, r_0 , of TP and TT

probe	S_0-S_2 (270 nm)	$S_0-S_1^a$	λ_{em} (nm) ^b
TP	-0.16	0.39	430–480
TT	-0.15	0.39	550–680

^a S_0-S_1 refers to an excitation wavelength of 420 nm for TP and 540 nm for TT. ^b Wavelength region over which the experimental values are averaged.

of degrees of freedom for the entire multidimensional fluorescence decay surface. Using $Z\chi_g^2$, the goodness of fits of analyses with different ν can be readily compared,

$$Z\chi_g^2 = \sqrt{\frac{\nu}{2}}(\chi_g^2 - 1) \quad (17)$$

Details and performance of the global analysis program are reported previously.²⁷ All global analyses are performed on an IBM RISC 6150-125 computer.

4. Results

A. General Properties of the Probes and Limiting Anisotropy of TP and TT. The fluorescence decays of TP and TT can be fitted to a monoexponential model under all experimental conditions. The fluorescence lifetimes of TT obtained by excitation at 270 nm are slightly, but systematically, higher than the fluorescence lifetimes obtained by excitation at 540 nm. A possible explanation can be given as follows. Since the quantum yield of TT is very high (0.95 in ethanol), the fluorescence decay time can be expected to be mainly determined by the radiative rate constant. This rate constant is inversely proportional to the index of refraction at the excitation wavelength,²⁹ which increases with decreasing wavelength. However, linking the fluorescence decay times over the excitation wavelengths hardly changes the values of the parameters of the anisotropy decay. Since the quantum yield of TP is lower (0.75 in ethanol), this effect is not observed for this compound.

The limiting anisotropy, r_0 , of TP and TT is determined by measuring the steady-state anisotropy in a viscous solvent (1,2-propanediol) at -60°C where rotational motions can be neglected. The values are reported in Table 2. The limiting anisotropy is calculated at each emission wavelength following eq 13 and then averaged over the indicated wavelength range.

Excitation in the visible band (S_0-S_1 transition) results in a high r_0 value, indicating that the transition dipoles for absorption and emission are almost parallel. In the UV region the angle between the dipoles is about $72^\circ-75^\circ$ as calculated from the experimentally determined value for r_0 . Since the absorption and emission spectra of the S_0-S_1 transition shift to the red by elongating the conjugated system in one direction, we assume that the transition dipoles for this transition are oriented along this direction. The position of the absorption spectra of the S_0-S_n transition is independent of the length of conjugation, and therefore the orientation of the transition dipole for absorption is mainly perpendicular to the axis of elongation. This is in agreement with the orientation of the transition dipoles found for perylene¹⁶ (see Figure 1).

B. Time-Resolved Anisotropy. The polarized fluorescence decays of TP and TT in a homologue series of n -alkanes and n -alcohols are measured at two excitation wavelengths (TP in alcohols at 270 and 423 nm, TP in alkanes at 270 nm, and TT at 270 and 540 nm in alcohols and alkanes). The data have been globally analyzed for each of the series by linking the values of β at the same excitation wavelength, while the values of ϕ are linked over the two excitation wavelengths for each solvent.

TABLE 3: Global Analysis of $r(t)$ of TP in Alcohols^a

solvent	viscosity (mPa s) ²⁴	τ (ns)	β	ϕ (ns)	ϕ/η (ns/(mPa s))
pentanol (270 nm)	3.76	4.54	-0.12	0.50	0.13
pentanol (423 nm)		4.60	0.34		
hexanol (270 nm)	5.48	4.60	-0.12	0.57	0.10
hexanol (423 nm)		4.44	0.34		
octanol (423 nm)	9	4.67	0.34	1.02	0.11
decanol(270 nm)	14.3	4.68	-0.12	1.49	0.10
decanol (423 nm)		4.73	0.34		
undecanol (423 nm)	17.2	4.52	0.34	1.89	0.11

^a Global χ_g^2 is 1.13, global $Z\chi_g^2$ is 10.08, $T = 291$ K, $\lambda_{exc} = 423$ or 270 nm as indicated in brackets, $\lambda_{em} = 520$ nm, the time increment is 26 and 29 ps/channel.

TABLE 4: Global Analysis of $r(t)$ of TP in Alkanes^a

solvent	viscosity (mPa s) ²⁵	τ (ns)	β	ϕ (ns)	ϕ/η (ns/(mPa s))
decane	0.925	4.37	-0.14	0.16	0.17
dodecane	1.503	4.58	-0.14	0.27	0.18
tetradecane	2.335	4.65	-0.14	0.39	0.17
hexadecane	3.474	4.59	-0.14	0.56	0.16

^a Global χ_g^2 is 1.08, global $Z\chi_g^2$ is 4.69, $T = 291$ K, $\lambda_{exc} = 270$ nm, $\lambda_{em} = 470$ nm, the time increment is 18 ps/channel.

TABLE 5: Global Analysis of $r(t)$ of TT in Alcohols^a

solvent	τ (ns)	β	ϕ (ns)	ϕ/η (ns/(mPa s))
ethanol (270 nm)	4.25	-0.12	0.32	0.24
ethanol (540 nm)	4.15	0.36		
pentanol (270 nm)	4.17	-0.12	0.94	0.25
pentanol (540 nm)	4.11	0.36		
hexanol(270 nm)	4.19	-0.12	1.17	0.21
hexanol (540 nm)	4.15	0.36		
decanol(270 nm)	4.38	-0.12	3.25	0.237
decanol (540 nm)	4.29	0.36		

^a Global χ_g^2 is 1.01, global $Z\chi_g^2$ is 8.45, $T = 291$ K, $\lambda_{exc} = 270$ or 540 nm as indicated in brackets, $\lambda_{em} = 620$ nm, the time increment is 25 and 14 ps/channel.

TABLE 6: Global Analysis of $r(t)$ of TT in Alkanes^a

solvent	τ (ns)	b	ϕ (ns)	ϕ/η (ns/mPa s)
decane (270 nm)	4.05	-0.12	0.29	0.31
decane (540 nm)	3.68	0.36		
dodecane (270 nm)	4.14	-0.12	0.45	0.29
dodecane (540 nm)	3.81	0.36		
tetradecane (270 nm)	4.10	-0.12	0.68	0.29
tetradecane (540 nm)	3.88	0.36		
hexadecane (270 nm)	4.17	-0.12	0.95	0.27
hexadecane (540 nm)	3.87	0.36		

^a Global χ_g^2 is 1.10, global $Z\chi_g^2$ is 8.04, $T = 291$ K, $\lambda_{exc} = 270$ or 540 nm as indicated in brackets, $\lambda_{em} = 620$ nm, the time increment is 20ps/channel for excitation at 540 nm and 18 ps/channel for excitation at 270 nm.

The obtained results of TP in alcohols and alkanes and TT in alcohols and alkanes are shown in Tables 3–6. The viscosities are from refs 30 and 31.

The results shown in Table 3 agree well with the values reported previously²⁸ where not all possible linkages are utilized for a subset of the currently considered set of decay traces.

Biexponential analysis of $r(t)$ without any constraint does not lead to an improvement of the fitting criteria. Moreover, the results are not realistic and depend strongly on the initial guesses. This indicates that a monoexponential model is sufficient to characterize $r(t)$ of TT in alkanes and alcohols.

C. Temperature Dependence. The anisotropy decay of TT in decanol and hexadecane is studied in the temperature range from 298 to 333 K. The value for the β parameter is linked

TABLE 7: Global Analysis of $r(t)$ of TT in Hexadecane at Different Temperatures^a

temp (°C)	η (mPa s) ²⁵	τ (ns)	ϕ_{exp} (ns)	ϕ_{DKS} (ns)
25	3.086	3.98	0.91	0.95
30	2.758	3.96	0.78	0.84
35	2.458	3.95	0.67	0.74
40	2.243	3.94	0.61	0.66
45	2.038	3.94	0.52	0.60
50	1.86	3.92	0.47	0.54
60	1.705	3.91	0.37	0.48

^a β is 0.36, global $Z\chi_g^2$ is 11.65, global χ_g^2 is 1.17, $\lambda_{exc} = 540$ nm, $\lambda_{em} = 620$ nm, and the time increment is 23 ps/channel.

TABLE 8: Global Analysis of $r(t)$ of TT in Decanol at Different Temperatures^a

temp (°C)	η (mPa s) ²⁴	τ (ns)	ϕ_{exp} (ns)	ϕ_{DKS} (ns)
25	11.8	4.11	2.60	2.7
30	9.78	4.11	2.16	2.3
35	8.32	4.09	1.69	2.0
40	6.75	4.08	1.44	1.7
45	5.95	4.07	1.24	1.5
50	4.86	4.07	1.03	1.2
60	3.63	4.04	0.75	0.94

^a β is 0.36, global $Z\chi_g^2$ is 8.78, global χ_g^2 is 1.13, $\lambda_{exc} = 540$ nm, $\lambda_{em} = 620$ nm, and the time increment is 23 ps/channel.

TABLE 9: Calculated Reduced Correlation Times for Different Molecular Shapes of TP and TT Assuming Sticking Boundary Conditions^a

probe/model	ϕ_{red}^a (ns/(mPa s))	ϕ_{red}^b (ns/(mPa s))
TP/sphere	0.124	
TP/prolate	0.135	0.145
TP/oblate	0.185	0.215
TT/sphere	0.155	
TT/prolate	0.201	0.176
TT/oblate	0.314	0.356

^a In the case of a prolate model the tabulated values correspond with the single rotational correlation time for the minimum and maximum value of the axial ratio (see text). In the case of the oblate model the rotational correlation times of the biexponential decay of $r(t)$ are given for a single value of the axial ratio (see text).

over the different temperatures. The results of global analysis are shown in Tables 7 and 8. From the tables it is observed that the fluorescence lifetime decreases slightly with increasing temperature in both solvents.

5. Discussion

A. The Shape of the Molecules. A monoexponential anisotropy decay can be observed for (a) a sphere, (b) a prolate molecule with a transition moment along the symmetry axis, and (c) an oblate molecule when D_{\perp} and D_{\parallel} are of similar magnitude. To estimate theoretically the rotational correlation times of the solutes, the volume and the axial ratio of the solute have to be known. The van der Waals volume is estimated from Edwards increments³² and is calculated to be 496 Å³ for TP and 601 Å³ for TT. These volumes allow to calculate the viscosity independent reduced rotational correlation times, ϕ_{red} , assuming sticking boundary conditions

$$\phi_{red} = \phi/\eta \quad (18)$$

The calculated value of ϕ_{red} for TP modeled as a sphere is comparable to the experimental values in alcohols but is lower than the values in alkanes (see Table 9). The reduced rotational correlation times for TT in alcohols as well as in alkanes are higher than the calculated one. Because the C factor in the SDE equation can never be larger than 1 for apolar probes, the spherical model has to be rejected for both compounds.

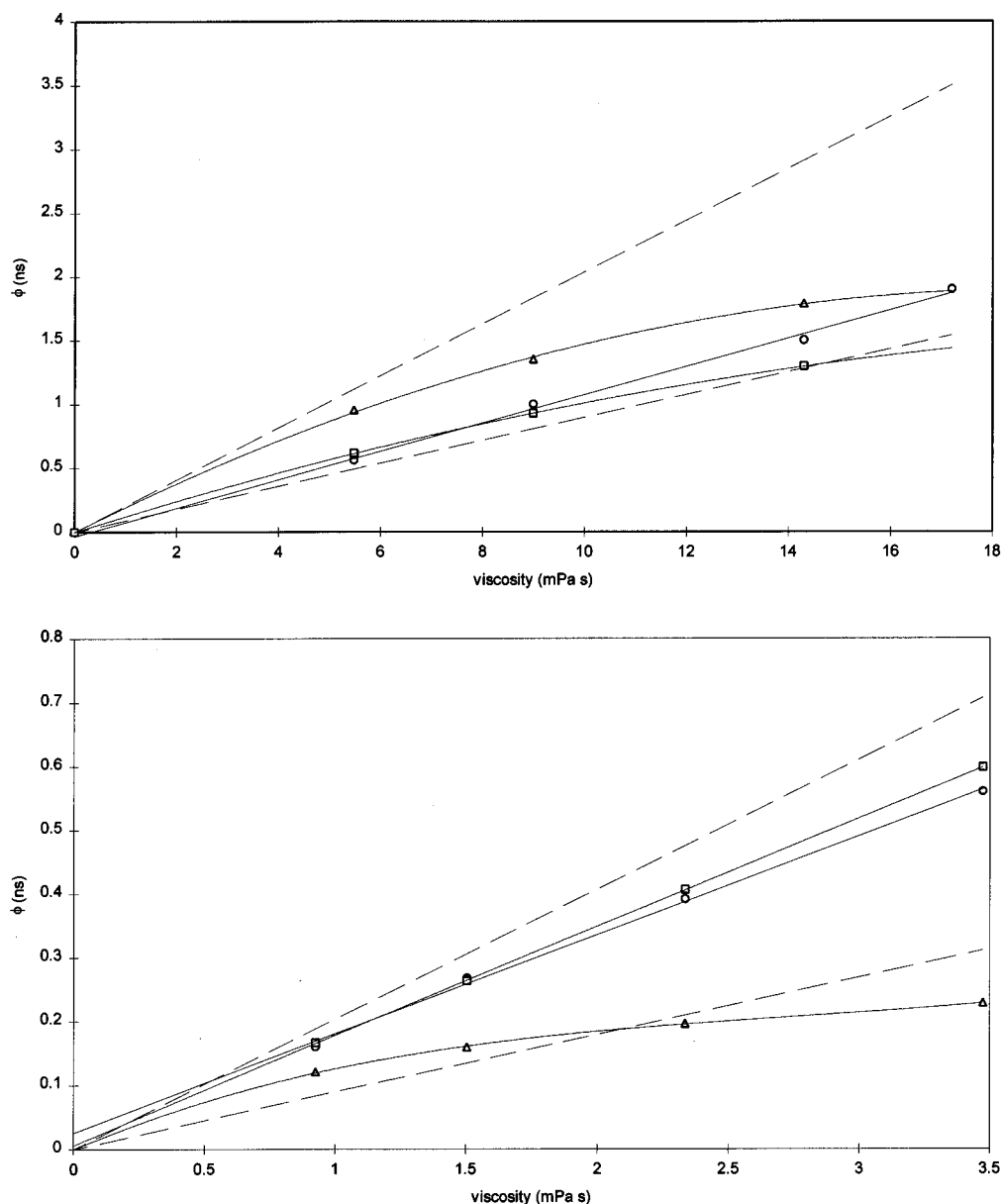


Figure 2. Comparison of experimental rotational correlation times (ϕ) of TP with rotational correlation times calculated according to hydrodynamic (slip and stick, ---) and quasihydrodynamic models of GW (Δ) and DKS (\square) in alcohols (a, top) and in alkanes (b, bottom).

TABLE 10: Activation Energies (in kcal/mol) for Viscosity (E_η) and for Rotation (E_{rot}) of TT in Hexadecane and Decanol

	E_η	E_{rot}
hexadecane	3.84	4.86
decanol	6.29	6.39

Both long axes in TP (i.e., the distance c–d and c–f in Figure 1) have the same length, indicating that a prolate molecule is not probable. Nevertheless, the theoretical reduced rotational correlation times for a prolate shape are calculated for both probes. Since it is quite difficult to estimate the actual axial ratio of TT, the extreme values of this parameter are calculated. The lower limit of the length of the long axis for TT is half of the distance a–b, while the upper limit is half of the distance c–d. The length of the minor axis is calculated from the van der Waals volume and the length of the major axis. This leads to an axial ratio between 1.71 and 1.44 and a corresponding shape factor of 1.14 and 1.3,²² respectively. The corresponding minimum and maximum values for the reduced rotational correlation times, ϕ_{red} , are given in Table 9. The same procedure is repeated for TP. For both probes the calculated values are lower than the experimentally determined values.

Therefore, we are forced to use an oblate model for TP and TT. In this model the distance from the center to the *tert*-butyl groups at the periphery of the molecules is taken as the length of the long axis (i.e., the distance d–e). The values for the short axes are calculated from the van der Waals volume and the length of the long axis. This leads to acceptable thicknesses of 4.6 Å for TP and 3.8 Å for TT, corresponding to axial ratios of 3.1 and 4.5 for TP and TT, respectively. Since molecules with an oblate shape show a biexponential anisotropy decay, both calculated rotational correlation times are given in Table 9. It can be seen that ϕ_{red}^a and ϕ_{red}^b differ not substantially. When the data are analyzed according to a biexponential anisotropy model, the recovered values for ϕ_1 and ϕ_2 are similar indeed. It can be concluded that D_\perp and D_\parallel are of similar magnitude. Also, the fitting criteria do not improve significantly for a biexponential model.

To check whether the program can discriminate between a biexponential and a monoexponential model with these relative values for the rotational correlation times, synthetic decays are generated with the calculated rotational correlation times for TT in decane at two excitation wavelengths (two sets of β 's), assuming sticking boundary conditions. These synthetic data

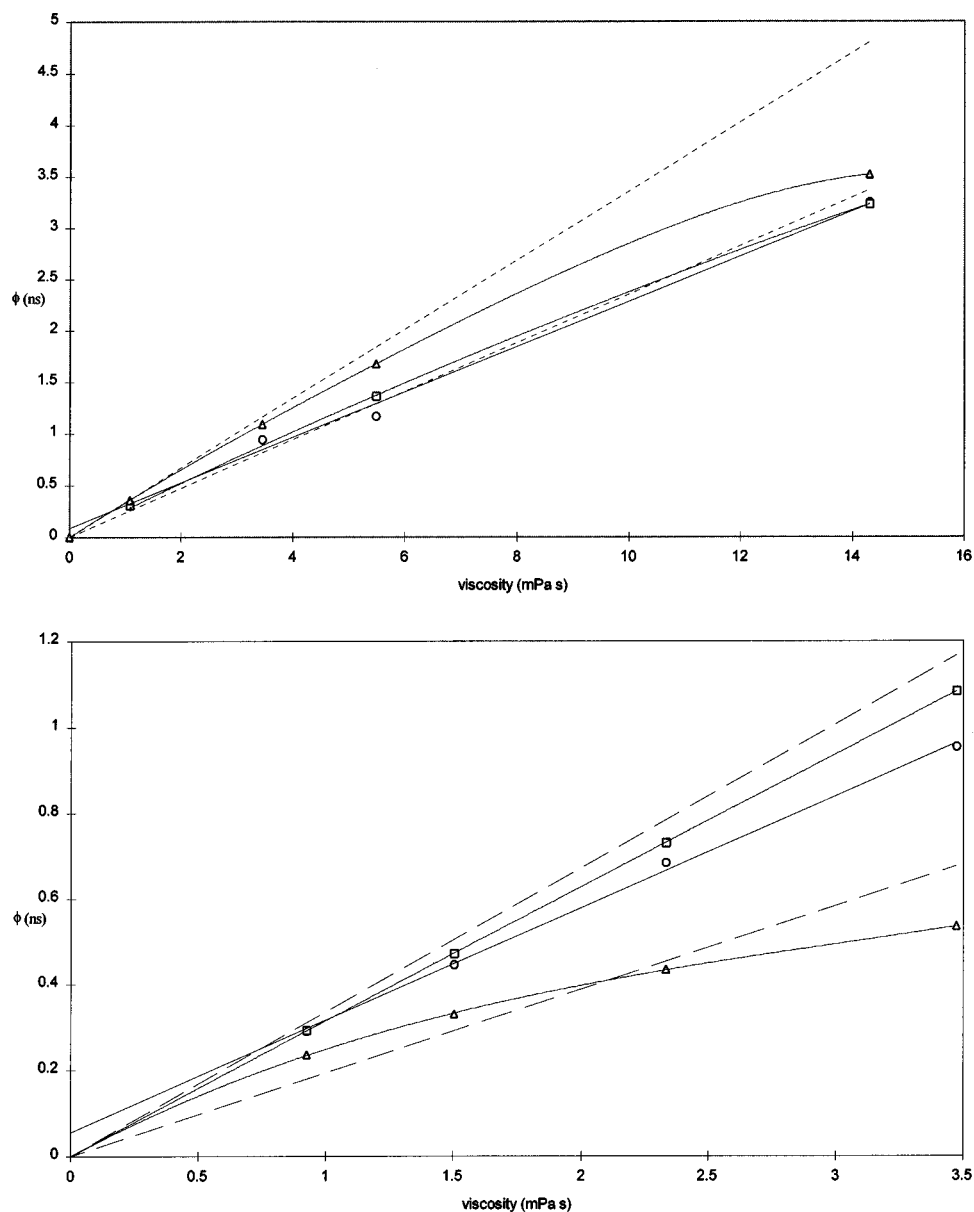


Figure 3. Comparison of experimental rotational correlation times (O) of TT with rotational correlation times calculated according to hydrodynamic (slip and stick, ---) and quasihydrodynamic models of GW (Δ) and DKS (\square) in alcohols (a, top) and alkanes (b, bottom).

are then analyzed as experimental data (results not shown). The simulations show that the program cannot recover the true parameters if no constraints are imposed. If β_1 is fixed to its true value of 0.1 (see eq 9), the rotational correlation times can be recovered. However, also analysis according to a monoexponential model gives statistical acceptable fits, indicating that a single rotational correlation time is sufficient to describe the rotational dynamics of TT. It may be noted that the obtained ϕ value for an analysis according to a monoexponential anisotropy model equals the experimentally observed ϕ value in decane. Further on a monoexponential anisotropy decay of TT in decane at two excitation wavelengths is simulated (results not shown). If these synthetic data are analyzed according to a monoexponential model, the correct values are obtained, as expected. If the data are analyzed according to a biexponential model with the constraint $\beta_1 = 0.1$, two slightly different ϕ values are obtained. These observations indicate that there is no justification to prefer the biexponential model above the monoexponential description.

The axial ratio of TP is closer to unity, resulting in even smaller differences between the two rotational correlation times. To obtain a more pronounced biexponential $r(t)$, it is necessary to further increase the difference between the long and short

axes. To this end we investigated 2,5,12,15-tetra-*tert*-butylquaterylene²⁶ (TQ in Figure 1) but failed due to the very low quantum yield of fluorescence and due to the poor sensitivity of the detection system of the single photon counting setup at the emission wavelength.

B. Solvent Dependence of the Rotational Correlation Times.

Since the molecules under investigation are neutral and apolar, no interference due to dielectric friction is expected. Therefore, the hydrodynamic stick or slip model is expected to give a constant value of the reduced rotational correlation times, ϕ_{red} , irrespective of the nature of the solvent. Consequently, any changes in ϕ_{red} in different isoviscous solvents are an indication of nonhydrodynamic effects. As expected from the SDE equation, a linear relation between viscosity and the ϕ values is observed in alkanes as well as in alcohols (see Figures 2 and 3). The values of the intercepts in comparison with an estimated experimental error of 30 ps do not allow us to attach a physical meaning to this parameter. The values of the rotational correlation times of both probes lay in between the slip and stick limits. The SDE relation predicts, however, the same reduced rotational correlation times in both solvent series. From the results in Tables 3–5 and the results of previous studies,^{13–15} one can see that this prediction does not hold at all. The reduced

rotational correlation times are lower for alcohols than for alkanes. This observation is an indication of a breakdown of the hydrodynamic theory. Since this theory is in principle only valid for macroscopic bodies in a continuum, the breakdown is more pronounced as the relative size of the solvent to the solute increases. In this context, it has to be mentioned that the difference between the correlation times is larger for TP than for TT. As mentioned in the Introduction, quasihydrodynamic theories (DKS and GW) try to take into account these size effects of solvent and solute. The molecular properties of the solvents and equations that are necessary to calculate the rotational correlation times following these quasihydrodynamical theories are taken from ref 10. The results of these calculations for TP and TT are shown in Figures 2 and 3. In all cases the DKS model gives a better description of the viscosity dependence of ϕ than the GW model.

C. Temperature Dependence. When the data from Tables 7 and 8 are plotted as a function of η/T , a straight line is obtained with the same characteristics as the lines of Figure 3. However, from Tables 7 and 8 it might be concluded that the experimental values for the rotational correlation times are slightly overestimated by the DKS model. It has been suggested in the literature³³ to interpret the temperature dependence of the rotational correlation times in terms of activation energies as follows. The temperature dependence of the viscosity is given by

$$\eta = \eta_0 \exp(E_\eta/RT) \quad (19)$$

where E_η is the viscosity activation energy. Combining this equation with the SDE equation leads to the following relation

$$\phi = \frac{\eta_0 V f C}{kT} \exp(E_\eta/RT) \quad (20)$$

Consequently, under the assumption of eq 1 plots of $\ln(T\phi)$ versus $1/T$ can be expected to be linear. Empirically the relation can be written as³³

$$\ln(T\phi) = A + (E_{\text{rot}}/RT) \quad (21)$$

where E_{rot} is the rotational activation energy. E_{rot} can be compared with E_η to test the hydrodynamic assumptions with respect to eq 1. Our data in hexadecane as well as the data from other authors^{33,34} reveal that E_{rot} is higher than E_η (Table 10). It has to be emphasized that the temperature study gives additional support to the DKS theory. The temperature dependence of ϕ is well described by DKS theory. In contrast to the SDE equation, the C factor in the DKS theory is temperature dependent. Therefore, it can be suggested that the discrepancy between E_{rot} and E_η is due to the fact that the SDE equation is inappropriate when solute and solvent molecules are of similar size.

6. Conclusions

The time-resolved anisotropy decay of two neutral and apolar molecules, TP and TT, are studied in alcohols and alkanes. The anisotropy decays of both molecules can be fitted to a monoexponential model. In spite of this model it is shown that these molecules cannot be seen as prolate or as spherical molecules, but as oblate ellipsoids with two indistinguishable rotational correlation times. The rotational correlation times of TP and TT are proportional to the viscosity for each solvent series. The rotation is for both probes faster in alcohols than in alkanes. This effect is more pronounced for TP than for TT, indicating that the SDE equation is not valid at a molecular scale. The quasihydrodynamic models of GW and DKS try to correct for

the solute and solvent size effects on this molecular scale. In spite of these corrections, only the DKS can predict qualitatively the experimental observations and explains the difference in rotational correlation times in terms of the higher free volume in alcohols than in alkanes.

The temperature study emphasizes the applicability of the DKS theory for nonpolar solutes and suggests that an Arrhenius formalism to calculate the activation energy for rotation from the SDE equation is not appropriate when solute and solvent molecules are of similar magnitude.

Acknowledgment. S.D.B. acknowledges the Vlaams Instituut voor de bevordering van het Wetenschappelijk Technologisch onderzoek in de industrie for a predoctoral fellowship. The continuing support of the Ministry of Scientific Programming (DWTC) through Grants UIAP-II-16 and IUAP-III-040 as well as the F.K.F.O. is gratefully acknowledged.

References and Notes

- (1) Perrin, F. *J. Phys. Radium* **1934**, 5, 497.
- (2) Hu, C.-M.; Zwanzig, R. *J. Chem. Phys.* **1974**, 60, 4354.
- (3) Youngren, G.; Acrivos, A. *J. Chem. Phys.* **1975**, 63, 3846.
- (4) Courtney, S. H.; Kim, S. K.; Canonica, S.; Fleming, G. R. *J. Chem. Soc., Faraday Trans. 2* **1986**, 82, 2065.
- (5) Canonica, S.; Schmid, A.; Wild, U. *Chem. Phys. Lett.* **1985**, 122, 529.
- (6) Gierer, A.; Wirtz, K. *Z. Naturforsch. A* **1953**, 8, 532.
- (7) Dote, J. L.; Kivelson, D.; Schwartz, R. *J. Phys. Chem.* **1981**, 85, 2169.
- (8) Alavi, D. S.; Hartman, R. S.; Waldeck D. H. *J. Chem. Phys.* **1991**, 94, 4509.
- (9) Sasaki, T.; Hirota, K.; Yamamoto, M.; Nishijima, Y. *Bull. Chem. Soc. Jpn.* **1987**, 60, 1165.
- (10) Justus, B.; Cox, A. J.; Butz, K. W.; Scott, G. W. *Chem. Phys.* **1988**, 119, 125.
- (11) Dutt, G. B.; Doraiswamy S.; Periasamy, N. *J. Chem. Phys.* **1991**, 94, 5360.
- (12) Williams, A. M.; Jiang, Y.; Ben-Amotz, D. *Chem. Phys.* **1994**, 180, 119.
- (13) Ben-Amotz, D.; Drake, J. M. *J. Chem. Phys.* **1988**, 89, 1019.
- (14) Ben-Amotz, D.; Scott, T. W. *J. Chem. Phys.* **1987**, 87, 3739.
- (15) Roy, M.; Doraiswamy, S. *J. Chem. Phys.* **1993**, 98, 3213.
- (16) Barkley, M.; Kowalczyk, A.; Brand, L. *J. Chem. Phys.* **1981**, 75, 3581.
- (17) Christensen, R. L.; Drake, R. C.; Phillips, D. *J. Phys. Chem.* **1986**, 90, 5960.
- (18) Piston, D.; Bilash, T.; Gratton, E. *J. Phys. Chem.* **1989**, 93, 3964.
- (19) Johansson, L. B. *J. Chem. Soc., Faraday Trans.* **1990**, 86, 2103.
- (20) Jiang, Y.; Blanchard, G. J. *J. Phys. Chem.* **1994**, 98, 6436.
- (21) Belford, G. G.; Belford R. L.; Weber G. *Proc. Natl. Acad. Sci. U.S.A.* **1972**, 69, 1392.
- (22) Small, E.; Isenberg, I. *Biopolymers* **1977**, 16, 1907.
- (23) Fleming, G. *Chemical Applications of Ultrafast Spectroscopy*; Oxford University: London, 1986.
- (24) Small, E. W.; Libertini, L. J.; Rudzki, K.; Small, J. In *Time-Resolved Laser Spectroscopy in Biochemistry*; Lakowicz, J. R., Ed.; S. P. I. E.: Bellingham, WA, 1988.
- (25) Lakowicz J. R. *Principles of Fluorescence Spectroscopy*; Plenum Press: New York, 1983.
- (26) Koch, K. H.; Mullen, K. *Chem. Ber.* **1991**, 124, 2091.
- (27) Crutzen, M.; Ameloot, M.; Boens, N.; Negri, R. M.; De Schryver, F. C. *J. Phys. Chem.* **1993**, 97, 8133.
- (28) De Backer, S.; Negri, R. M.; De Feyter, S.; Dutt, G. B.; Ameloot, M.; De Schryver, F. C.; Müllen, K.; Holtrup, F. *Chem. Phys. Lett.* **1995**, 233, 538.
- (29) Birks, J. B. *Photophysics of Aromatic Molecules*; 1970; p 88.
- (30) *Landolt-Börnstein Zahlenwerte und funktionen*; Springer-Verlag: Berlin, 1969; Band II, Teil 5.
- (31) *Selected Values of Physical and Thermodynamic properties of Hydrocarbons and Related Compounds*; Carnegie Press: Pittsburgh, PA, 1953.
- (32) Edward, J. T. *J. Chem. Educ.* **1970**, 47, 261.
- (33) Bessire, D. R.; Quitevis, E. L. *J. Chem. Phys.* **1994**, 98, 13083.
- (34) Waldeck, D.; Fleming, G. *J. Phys. Chem.* **1981**, 85, 2614.